ELSEVIER
Comput. Methods Appl. Mech. Engrg. 183 (2000) 123–140
Computer methods in applied mechanics and engineering
www.elsevier.com/locate/cma

Interaction of deformation waves and localization phenomena in inelastic solids

Adam Glema [a], Tomasz Łodygowski [a], Piotr Perzyna [a,b,*]

[a] Institute of Structural Engineering, Poznań University of Technology, ul.Piotrowo 5, 60-965 Poznań, Poland
[b] Centre of Mechanics, Institute of Fundamental Technological Research, Polish Academy of Sciences, Świetokrzyska 21, 00-049 Warsaw, Poland

Abstract

The main objective of this paper is the investigation of the interaction and reflection of elastic–viscoplastic waves which can lead to localization phenomena in solids. The rate type constitutive structure for an elastic–viscoplastic material with thermomechanical coupling is developed. An adiabatic inelastic flow process is considered. The Cauchy problem is investigated and the conditions for well-posedness are examined. Discussion of fundamental features of rate-dependent plastic medium is presented. This medium has dissipative and dispersive properties. Mathematical analysis of the evolution problem (the dynamical initial-boundary value problem) is presented. The dispersion property implies that in the viscoplastic medium any initial disturbance can break up into a system of group of oscillations or wavelets. On the other hand, the dissipation property causes the amplitude of a harmonic wavetrain to decay with time. In the evolution problem considered in such dissipative and dispersive medium, the stress and deformation due to wave reflections and interactions are not uniformly distributed, and this kind of heterogeneity can lead to strain localization in the absence of geometrical or material imperfections.

Since the rate-independent plastic response is obtained as the limit case, when the relaxation time T_m tends to zero, the theory of viscoplasticity offers the regularization procedure for the numerical solution of the dynamical initial-boundary value problems with localization of plastic deformation.

Numerical examples are presented for a steel bar axisymmetric specimen subjected to tension, with the controlled displacements imposed at one or two opposite sides with different velocities. Two cases of the initial-boundary conditions are considered; (A) symmetric (double side) tension of the specimen which results in symmetric pattern of deformations; (B) asymmetric (single side) tension of the specimen with the opposite side fixed, which leads to non-symmetric deformation.

For both cases of boundary conditions a set of examples is computed with different initial velocities changing between 0.5 and 20 m/s. The final states are defined by prescribed value of the total elongation of a specimen. In the numerical examples the attention is focused on the investigation of the interactions and reflections of waves and on the location of localization of plastic deformation. The distribution of plastic equivalent strain, temperature and vector plots of velocities represents the results. The computations are performed using the industrial finite element program ABAQUS (explicit method).

1. Introduction

The correspondence between stationary body waves and bulk localization has long been appreciated (cf. [9,49,10,51,18,40]). In many recently published papers the investigation of adiabatic shear band localization phenomena has been based on an analysis of acceleration waves and has taken advantage of a notion of the instantaneous adiabatic acoustic tensor (cf. [3–5,26,31,40,50]). Connection between stationary waves, stability and well-posedness of initial-boundary value problems has received considerable attention (cf. Simpson and Spector (1987), [43,2,25]). The analysis of the influence of the effect of boundaries and interfaces on shear band localization in time- and rate-independent plastic materials has been based on the

* Corresponding author.

0045-7825/00/$ - see front matter
PII: S 0 0 4 5 - 7 8 2 5 (9 9) 0 0 2 1 5 - 7

investigation of stationary body, Rayleigh and Stoneley waves (cf. [22,47]). They defined stability, in the sense of limits to the uniqueness of solutions to quasi-static boundary value problems and addressed stability in terms of the existence of certain stationary waves.

Very recently, it has been widely recognized to consider an elastic–viscoplastic model of a material as a regularization method for solving mesh-dependent strain softening problems of plasticity (cf. [6,7,14–17,20,21,23,24,31–35,37,44,45,52,53]).

In these regularized initial-boundary value problems, wave propagation phenomena play a fundamental role. Since an elastic–viscoplastic model introduces dissipative as well as dispersive nature for the propagated waves, the analysis of dispersive, dissipative waves and particularly their interactions and reflections have to be considered as the most important problem. The main objective of the present paper is the investigation of the interaction and reflection of elastic–viscoplastic waves which can lead to localization of plastic deformation in solids.

In Section 2 the rate type constitutive structure for an elastic–viscoplastic material with thermomechanical coupling is developed. Section 3 is devoted to the formulation and investigation of an adiabatic inelastic flow process. The Cauchy problem is investigated and the conditions which guarantee its well-posedness are examined.

In Section 4 the dispersive analysis of the evolution problem is presented. First, the linear case of the evolution problem is considered. A particular wave solution by the simple harmonic wavetrains is investigated. The dispersion relation, the phase and group velocities are determined and main dispersive properties are discussed. Second, the discussion of fundamental features of rate-dependent medium is presented. Numerical solutions of the initial-boundary value problem (evolution problem) are discussed in Section 5. Mathematical formulation of the evolution problem is presented. Discretization in space and time is proposed and convergence, consistency and stability are examined. The Lax–Richtmayer equivalence theorem is formulated and conditions under which this theorem is valid are investigated.

In Section 6 numerical examples are presented for a steel bar axisymmetric specimen subjected to tension, with the controlled displacements imposed at one or two opposite sides with different velocities. Two cases of the initial-boundary conditions are considered; (A) symmetric (double side) tension of the specimen which results in symmetric pattern of deformations; (B) asymmetric (single side) tension of the specimen with the opposite side fixed, which leads to non-symmetric deformation. For both cases of boundary conditions a set of examples is computed with different initial velocities changing between 0.5 and 20 m/s. The final states are defined by the prescribed value of the total elongation of a specimen.

Numerical examples clearly show that the localization of plastic deformation is generated by the interactions and reflections of dispersive, dissipative waves.

In Section 7 main final comments are presented.

2. Constitutive structure for thermoviscoplasticity

The main objective is to develop the rate type constitutive structure for an elastic–viscoplastic material in which the effects of thermomechanical couplings are taken into consideration.

Let us introduce the axioms as follows:

(i) Axiom of the existence of the free energy function in the form

$$\psi = \hat{\psi}(\mathbf{e}, \mathbf{F}, \vartheta; \boldsymbol{\mu}), \tag{1}$$

where $\mathbf{e}$ is the Eulerian strain tensor, $\mathbf{F}$ the deformation gradient, ϑ a temperature field and $\boldsymbol{\mu}$ denotes the internal state variable vector.

(ii) *Axiom of objectivity* (spatial covariance). The constitutive structure should be invariant with respect to any diffeomorphism $\boldsymbol{\xi} : \mathscr{S} \to \mathscr{S}$, where $\mathscr{S}$ denotes the actual (spatial) configuration of a body $\mathscr{B}$, cf. [19].

(iii) *The axiom of entropy production*. For any regular process ϕ_t, ϑ_t, $\boldsymbol{\mu}_t$ of a body $\mathscr{B}$ the constitutive functions are assumed to satisfy the reduced dissipation inequality

$$\frac{1}{\rho_{\mathrm{Ref}}}\boldsymbol{\tau}:\mathbf{d}-(\eta\dot{\vartheta}+\dot{\psi})-\frac{1}{\rho\vartheta}\mathbf{q}\cdot\operatorname{grad}\vartheta\geqslant 0, \tag{2}$$

where ρ and ρ_{Ref} denote the mass density in the actual and reference configuration, respectively, $\boldsymbol{\tau}$ the Kirchhoff stress tensor, $\mathbf{d}=\mathbf{d}^e+\mathbf{d}^p$ the rate of total deformation, η denotes the specific (per unit mass) entropy and $\mathbf{q}$ is the heat vector field.

Let us postulate $\boldsymbol{\mu}=\in^p$, where $\in^p=\int_0^t\left(\frac{2}{3}\mathbf{d}^p:\mathbf{d}^p\right)^{1/2}\,\mathrm{d}t$ is the equivalent plastic deformation. It is introduced as the internal state variable to describe the dissipation effects generated by viscoplastic flow phenomena.

Let us assume the plastic potential function for a material in the form

$$f=J_2,\quad \text{where } J_2=\frac{1}{2}\tau'^{ab}\tau'^{cd}g_{ac}g_{bd}, \tag{3}$$

and $\mathbf{g}$ denotes the metric tensor in $\mathscr{S}$.

Let us postulate the evolution equation as follows:

$$\mathbf{d}^p=\Lambda\mathbf{P}, \tag{4}$$

where for the elastic–viscoplastic model of a material we assume (cf. [27,28,31–33])

$$\Lambda=\frac{1}{T_{\mathrm{m}}}\left\langle\Phi\left(\frac{f}{\kappa}-1\right)\right\rangle. \tag{5}$$

T_{m} denotes the relaxation time for mechanical disturbances and κ is the isotropic work-hardening parameter, Φ the empirical overstress function and the bracket $\langle\cdot\rangle$ defines the ramp function, $\mathbf{P}=(1/2\sqrt{J_2})(\partial f/\partial\boldsymbol{\tau})$. Thus, we have

$$P_{ab}=\frac{1}{2\sqrt{J_2}}\tau'^{cd}g_{ca}g_{db}. \tag{6}$$

The isotropic hardening–softening material function κ is assumed in the form as follows:

$$\kappa=\kappa_0^2\{q+(1-q)\exp\left[-h(\vartheta)\in^p\right]\}^2(1-b\vartheta), \tag{7}$$

where $q=\kappa_1/\kappa_0$, κ_0 and κ_1 denote the yield and saturation stress of the matrix material, respectively, $h=h(\vartheta)$ is the temperature-dependent strain hardening function for the matrix material and b is a material coefficient. The overstress viscoplastic function Φ is postulated in the form (cf. [27–30])

$$\Phi\left(\frac{f}{\kappa}-1\right)=\left(\frac{f}{\kappa}-1\right)^m,\quad \text{where } m=1,3,5,\ldots \tag{8}$$

The axioms (i)–(iii) and the evolution equations (4) lead to the rate equations as follows:

$$\begin{gathered}\mathrm{L}_v\boldsymbol{\tau}=\mathscr{L}^e:\mathbf{d}-\mathscr{L}^{\mathrm{th}}\dot{\vartheta}-[(\mathscr{L}^e+\mathbf{g}\boldsymbol{\tau}+\boldsymbol{\tau}\mathbf{g}):\mathbf{P}]\frac{1}{T_m}\left\langle\Phi\left(\frac{f}{\kappa}-1\right)^m\right\rangle,\\ \dot{\vartheta}=-\frac{1}{\rho c_p}\operatorname{div}\mathbf{q}+\frac{\vartheta}{c_p\rho_{\mathrm{Ref}}}\frac{\partial\boldsymbol{\tau}}{\partial\vartheta}:\mathbf{d}+\frac{\chi}{\rho c_p}\boldsymbol{\tau}:\mathbf{d}^p,\end{gathered} \tag{9}$$

where L_v defines the Lie derivative with respect to the velocity field, dot denotes the material derivative and ρ is the actual density,

$$\mathscr{L}^e=\rho_{\mathrm{Ref}}\frac{\partial^2\hat{\psi}}{\partial\mathbf{e}^2},\quad \mathscr{L}^{\mathrm{th}}=-\rho_{\mathrm{Ref}}\frac{\partial^2\hat{\psi}}{\partial\mathbf{e}\partial\vartheta},\quad c_p=-\vartheta\frac{\partial^2\hat{\psi}}{\partial\vartheta^2}, \tag{10}$$

χ is the irreversibility coefficient.

To make possible numerical investigation of the three-dimensional dynamic adiabatic deformations of a body for different ranges of strain rate we introduce some simplifications of the constitutive model. The infinitesimal linear theory of elasticity is postulated with G and K as the shear and bulk modulus, respectively.

3. Adiabatic inelastic flow process

3.1. Formulation of an adiabatic inelastic flow process

Let us define an adiabatic inelastic flow process as follows (cf. [31–33]). Find ϕ, $\boldsymbol{v}$, ρ, $\boldsymbol{\tau}$ and ϑ as functions of t and $\mathbf{x}$ such that

(i) the field equations

$$\dot{\boldsymbol{\varphi}} = \mathscr{A}(t, \mathbf{x}, \boldsymbol{\varphi})\boldsymbol{\varphi} + \mathbf{f}(t, \mathbf{x}, \boldsymbol{\varphi}), \tag{11}$$

where

$$\boldsymbol{\varphi} = \begin{bmatrix} \phi \\ \boldsymbol{v} \\ \rho \\ \boldsymbol{\tau} \\ \vartheta \end{bmatrix}, \quad \mathbf{f} = \begin{bmatrix} \boldsymbol{v} \\ 0 \\ 0 \\ -\left[\left(\mathscr{L}^{\mathrm{th}} \frac{\chi}{\rho c_p}\boldsymbol{\tau} + \mathscr{L}^e + \mathbf{g}\boldsymbol{\tau} + \boldsymbol{\tau}\mathbf{g}\right) : \mathbf{P}\right] \frac{1}{T_m} \langle \Phi(\frac{f}{\kappa} - 1)\rangle \\ \frac{\chi}{\rho c_p}\boldsymbol{\tau} : \mathbf{P}\frac{1}{T_m}\langle \Phi(\frac{f}{\kappa} - 1)\rangle \end{bmatrix},$$
$$\mathscr{A} = \begin{bmatrix} 0 & 0 & 0 & 0 & 0 \\ 0 & 0 & \frac{\tau}{\rho_{\mathrm{Ref}}\rho}\mathrm{grad} & \frac{1}{\rho_{\mathrm{Ref}}}\mathrm{div} & 0 \\ 0 & -\rho\mathrm{div} & 0 & 0 & 0 \\ 0 & \mathscr{L}^e : \mathrm{sym}\frac{\partial}{\partial \mathbf{x}} + 2\,\mathrm{sym}\left(\boldsymbol{\tau} : \frac{\partial}{\partial \mathbf{x}}\right) & 0 & 0 & 0 \\ 0 & 0 & 0 & 0 & 0 \end{bmatrix}; \tag{12}$$

(ii) the boundary conditions

(a) displacement ϕ is prescribed on a part ∂_ϕ of $\partial\phi(\mathscr{B})$ and tractions $(\boldsymbol{\tau} \cdot \mathbf{n})^a$ are prescribed on part ∂_τ of $\partial\phi(\mathscr{B})$, where $\partial_\phi \cap \partial_\tau = 0$ and $\overline{\partial_\phi \cup \partial_\tau} = \partial\phi(\mathscr{B})$;

(b) heat flux $\mathbf{q} \cdot \mathbf{n} = 0$ is prescribed on $\partial\phi(\mathscr{B})$;

(iii) the initial conditions ϕ, $\boldsymbol{v}$, ρ, $\boldsymbol{\tau}$ and ϑ are given at each particle $X \in \mathscr{B}$ at $t = 0$;

are satisfied.

In Eq. (12) $\partial\boldsymbol{v}/\partial\mathbf{x}$ defines the spatial velocity gradient and ρ_{Ref} denotes density in the reference configuration.

3.2. The Cauchy problem

Let us consider the Cauchy problem

$$\dot{\boldsymbol{\varphi}} = \mathscr{A}(t, \boldsymbol{\varphi})\boldsymbol{\varphi} + \mathbf{f}(t, \boldsymbol{\varphi}), \quad t \in [0, t_f], \ \ \boldsymbol{\varphi}(0) = \boldsymbol{\varphi}^0, \tag{13}$$

where $\mathscr{A}$ is a spatial differential operator and $\mathbf{f}$ is a non-linear function, both defined by (12), (cf. [31–33]).

In order to examine the existence, uniqueness and well-posedness of the Cauchy problem (13) let us assume that the spatial differential operator $\mathscr{A}$ has domain $\mathscr{D}(\mathscr{A})$ and range $\mathscr{R}(\mathscr{A})$, both contained in a real Banach space E and the non-linear function $\mathbf{f}$ is as follows $\mathbf{f} : E \to E$. To investigate the existence as well as the stability of solutions to (13) it is necessary to characterize their properties without actually constructing the solutions. This can be done by considering the properties of a non-linear semi-group because if the operator $\mathscr{A} + \mathbf{f}(\cdot)$ generates a non-linear semi-group $\{\mathbb{F}_t^*; t \geqslant 0\}$, then a solution to (13) starting at $t = 0$ from any element $\boldsymbol{\varphi}^0 \in \mathscr{D}(\mathscr{A})$ is given by

$$\boldsymbol{\varphi}(t, \mathbf{x}) = \mathbb{F}_t^* \boldsymbol{\varphi}^0(\mathbf{x}) \quad \text{for } t \in [0, t_f]. \tag{14}$$

We say the problem (13) is well posed if $\mathbb{F}_t^*$ is continuous (in the topology on $\mathscr{D}(\mathscr{A})$ and $\mathscr{R}(\mathscr{A})$ assumed) for each $t \in [0, t_f]$.

Let us postulate as follows:
(i) the strong ellipticity condition in the form:

$$\mathbb{E} = \mathscr{L}^e - \frac{1}{c_p \rho_{\mathrm{Ref}}} \vartheta \mathscr{L}^{\mathrm{th}} \frac{\partial \boldsymbol{\tau}}{\partial \vartheta} \tag{15}$$

is strongly elliptic (at a particular deformation ϕ) if there is an $\epsilon > 0$ such that

$$\mathbb{E}^{abcd} \zeta_a \zeta_c \xi_b \xi_d \geqslant \epsilon \|\boldsymbol{\zeta}\|^2 \ \|\boldsymbol{\xi}\|^2 \tag{16}$$

for all vectors $\boldsymbol{\zeta}$ and $\boldsymbol{\xi} \in \mathbb{R}^3$;
(ii) for positive numbers $\lambda_{\mathbf{f}}^1$ and $\lambda_{\mathbf{f}}^2$ and for $T_m > 0$

$$\mathbf{f}(t, \boldsymbol{\varphi}) \in E, \quad \|\mathbf{f}(t, \boldsymbol{\varphi})\|_E \leqslant \lambda_{\mathbf{f}}^1, \quad \|\mathbf{f}(t, \boldsymbol{\varphi}') - \mathbf{f}(t, \boldsymbol{\varphi})\|_E \leqslant \lambda_{\mathbf{f}}^2 \|\boldsymbol{\varphi}' - \boldsymbol{\varphi}\|_E \tag{17}$$

and

$$t \to \mathbf{f}(t, \boldsymbol{\varphi}) \in E \text{ is continuous.} \tag{18}$$

Using the results presented by Hughes et al. [11] and Marsden and Hughes [19] it is possible to show (cf. [31–33]) that the conditions (i) and (ii) guarantee the existence of (locally defined) evolution operators $\mathbb{F}_t^* : E \to E$ that are continuous in all variables. In other words the solution of the Cauchy problem (13) in the form (14) exists, is unique and well-posed.

4. Mathematical analysis of the evolution problem

4.1. Dispersive analysis

As a matter of fact, the dispersion of a waveform is caused by certain physical and/or geometrical characteristics of the medium in which the wave is generated. Consequently, instead of dispersive waves, it is perhaps more precise to speak of *a dispersive medium* or, where geometrical features alone cause the dispersion, *a dispersive geometry*, cf. [48].

The relaxation time T_m (or viscosity) can be viewed either as a regularization parameter or as a microstructural parameter to be determined from experimental observations.

To make our analysis easier let us consider the linear, dispersive, non-dissipative system of equations

$$\dot{\boldsymbol{\varphi}} = \mathscr{A}_0^{\star}(t, \mathbf{x}) \boldsymbol{\varphi} + f_0^{\star}(t, \mathbf{x}) \boldsymbol{\varphi}. \tag{19}$$

The theory of dispersive wave propagation can be introduced by a particular wave solution of Eq. (19), namely, by the simple harmonic wavetrains (cf. [54,55,48])

$$\boldsymbol{\varphi} = A \exp[\mathrm{i}(\mathbf{k} \cdot \mathbf{x} - \omega t)], \tag{20}$$

where $\mathbf{k}$ is the wave number, ω the frequency, and A denotes the amplitude.

Since a set of equations (19) is linear, A factors out and can be arbitrary. To satisfy a set of equations (19), $\mathbf{k}$ and ω have to be related by an equation

$$G(\omega, \mathbf{k}, \mathbf{x}, t) = 0, \tag{21}$$

which is called the dispersion relation.

Let us assume that the dispersion relation may be solved in the form of real roots

$$\omega = W(\mathbf{k}, \mathbf{x}, t). \tag{22}$$

There will be a number of such solutions, in general, with different functions $W(\mathbf{k}, \mathbf{x}, t)$. We refer to these as different modes.

The phase velocity $\mathbf{c}$ is given as a function of wavenumber

$$\mathbf{c}(\mathbf{k}, \mathbf{x}, t) = \frac{\omega}{k} \hat{\mathbf{k}} = k^{-1} W(\mathbf{k}, \mathbf{x}, t) \hat{\mathbf{k}}, \tag{23}$$

where $\hat{\mathbf{k}}$ is the unit vector in the $\mathbf{k}$ direction. For any particular mode $\omega = W(\mathbf{k}, \mathbf{x}, t)$, the phase velocity $\mathbf{c}$ is a function of $\mathbf{k}$.

Another velocity associated with the harmonic wavetrains (20) in dispersive media is the group velocity $\mathbf{C}$ defined as

$$\mathbf{C}(\mathbf{k}, \mathbf{x}, t) = \frac{\partial W(\mathbf{k}, \mathbf{x}, t)}{\partial \mathbf{k}}, \tag{24}$$

which also depends on the wavenumber $\mathbf{k}$.

The derivative of $\mathbf{C}$ with respect to $\mathbf{k}$ is the symmetric dispersive tensor

$$W_{\mathbf{kk}} = \frac{\partial^2 W}{\partial \mathbf{k}^2}. \tag{25}$$

To have dispersive waves we have to introduce two assertions:

$$\text{(i)}\ W(\mathbf{k}, \mathbf{x}, t)\ \text{is real;} \tag{26}$$

$$\text{(ii)}\ \det \left| \frac{\partial^2 W}{\partial k_i \partial k_j} \right| \neq 0.$$

The second condition of (26) ensures that the group velocity $\mathbf{C}$ is not a constant.

The quantity

$$\theta = \mathbf{k} \cdot \mathbf{x} - \omega t \tag{27}$$

in the solution (20) is the phase.

The group velocity is actually the most important velocity associated with dispersive waves, as it not only is the velocity of a given group of oscillations or 'wavelets' in a wavetrain but also coincides with the velocity with which the energy in that group propagates. Moreover, in a dispersive medium any initial disturbance is eventually broken up into a system of such groups.

Since the medium under consideration also has dissipation property (cf. Eq. $(9)_2$ in which the last term on the right-hand side is responsible for dissipation effect) hence mathematically, loses due to dissipation are manifested by the dispersion relation yielding complex or pure imaginary values of W corresponding to real values of $\mathbf{k}$. The amplitude of a harmonic wavetrain then decays exponentially with time.

If the dissipation becomes appreciable, as is in the elastic–viscoplastic medium, then the general theory of waves in dispersive media would require modification. [1]

The previous consideration does not apply to the general non-linear case (cf. Eq. (11)). To obtain some results we can use the variational method, the perturbation theory or the numerical finite element procedure.

4.2. Fundamental features of the rate-dependent plastic model

It has been proved that the localization of plastic deformation phenomenon in an elastic-viscoplastic solid body can arise only as the result of the reflection and interaction of waves. It has a different character than that which occurs in a rate-independent elasto-plastic solid body (cf. [31–33]). Rate dependency (viscosity) allows the spatial difference operator in the governing equations to retain its ellipticity and the initial value problem is well-posed. Viscosity introduces implicitly a length-scale parameter into the dynamical initial-boundary value problem and hence it implies that the localization region is diffused when compared with an inviscid plastic material. In the dynamical initial-boundary value problem the stress and deformation due to wave reflections and interactions are not uniformly distributed, and this kind of heterogeneity can lead to strain localization in the absence of geometrical or material irregularities. This kind of phenomenon has been recently noticed by Nemes and Eftis [23] (cf. also the results by Sluys et al. [45]).

[1] Examples of some solutions of linear, one-dimensional wave propagation problems in an elstic–viscoplastic medium have been recently proposed, cf. [45,44,53,52,36]).

The theory of viscoplasticity gives the possibility to obtain mesh-insensitive results in localization problems with respect to the width of the shear band and the wave reflection and interaction patterns (cf. [45]).

Since the rate-independent plastic response is obtained as the limit case when the relaxation time T_m tends to zero (cf. [31–33]) the theory of viscoplasticity offers the regularization procedure for the solution of the dynamical initial-boundary value problems with localization of plastic deformation.

However the most important feature is that the propagation of deformation waves in an elastic–viscoplastic medium has dispersive nature.

In this paper we shall use the numerical finite element procedure to show the solution of the particular evolution problems with non-linear dissipative and dispersive wave effects.

The application of the variational method and the perturbation theory in the investigation of the non-linear evolution problems will be presented by the authors in the forthcoming papers.

5. Numerical solution of the initial-boundary value problem (evolution problem)

5.1. Formulation of the evolution problem

Find $\boldsymbol{\varphi}$ as function of t and $\mathbf{x}$ satisfying [2]

(i) $\dot{\boldsymbol{\varphi}} = \mathscr{A}(t, \boldsymbol{\varphi})\boldsymbol{\varphi} + \mathbf{f}(t, \boldsymbol{\varphi})$;

(ii) $\boldsymbol{\varphi}(0) = \boldsymbol{\varphi}^0(\mathbf{x})$; (28)

(iii) The boundary conditions (e.g. as have been postulated in Section 3.1).

A strict solution of (28) with $\mathbf{f}(t, \boldsymbol{\varphi}) \equiv 0$ (i.e. the homogeneous evolution problem) is defined as a function $\boldsymbol{\varphi}(t) \in E$ (a Banach space) such that

$$\boldsymbol{\varphi}(t) \in \mathscr{D}(\mathscr{A}) \quad \text{for all } t \in [0, t_f],$$
$$\lim_{\Delta t \to 0} \left\| \frac{\boldsymbol{\varphi}(t + \Delta t) - \boldsymbol{\varphi}(t)}{\Delta t} - \mathscr{A}\boldsymbol{\varphi}(t) \right\|_E = 0 \quad \text{for all } t \in [0, t_f]. \tag{29}$$

The boundary conditions are taken care of by restricting the domain $\mathscr{D}(\mathscr{A})$ to elements of E that satisfy those conditions; they are assumed to be linear and homogeneous, so that the set $\mathbf{S}$ of all $\boldsymbol{\varphi}$ that satisfy them is a linear manifold; $\mathscr{D}(\mathscr{A})$ is assumed to be contained in $\mathbf{S}$.

The choice of the Banach space E, as well as the domain of $\mathscr{A}$, is an essential part of the formulation of the evolution problem.

5.2. Well-posedness of the evolution problem

The homogeneous evolution problem (i.e. for $\mathbf{f} \equiv 0$) is called well-posed (in the sense of Hadamard) if it has the following properties:

(i) The strict solutions are uniquely determined by their initial elements;

(ii) The set Y of all initial elements of strict solutions is dense in the Banach space E;

(iii) For any finite interval $[0, t_0]$, $t_0 \in [0, t_f]$ there is a constant $K = K(t_0)$ such that every strict solution satisfies the inequality

$$\|\boldsymbol{\varphi}(t)\| \leqslant K\|\boldsymbol{\varphi}^0\| \quad \text{for } 0 \leqslant t \leqslant t_0. \tag{30}$$

The inhomogeneous evolution problem (28) will be called well posed if it has a unique solution for all reasonable choices of $\boldsymbol{\varphi}^0$ and $\mathbf{f}(t, \boldsymbol{\varphi})$ and if the solution depends continuously, in some sense, on those choices.

[2] We shall follow here some fundamental results which have been discussed in [42,46,41,13,1,8].

It is possible to show (cf. [41]) that strict solutions exist for sets of $\boldsymbol{\varphi}^0$ and $\mathbf{f}(\cdot)$ that are dense in E and E_1 (a new Banach space), respectively.

5.3. Discretisation in space and time

We must approximate (28) twice. First, when E is infinite dimensional, we must replace $\mathscr{A}$ by an operator $\mathscr{A}_h$ which operates in a finite dimensional space $V_h \subset E$, where, in general, $h > 0$ represents a discretization step in space, such that $\dim(V_h) \to \infty$ as $h \to 0$. Second, we must discretize in time, that is to say choose a sequence of moments t_n (for example $t_n = n\Delta t$, where Δt is time step) at which we shall calculate the approximate solution.

Let us introduce the following semi-discretized (discrete in space) problem.

$$\begin{aligned}&\text{Find } \boldsymbol{\varphi}_h \in \mathscr{C}^0([0,t_0];V_h)\ (\mathscr{C}^0 \text{denotes the space of functions}\\ &\quad \text{continuous on } ([0,t_0],V_h)) \text{ satisfying}\\ &\frac{\mathrm{d}\boldsymbol{\varphi}_h(t)}{\mathrm{d}t} = \mathscr{A}_h\boldsymbol{\varphi}_h(t) + \mathbf{f}_h(t), \quad \boldsymbol{\varphi}_h(0) = \boldsymbol{\varphi}_{0,h}.\end{aligned} \tag{31}$$

The operator $\mathscr{A}_h$ for the finite element method can be obtained by a variational formulation approach. The discrete equations are obtained by the Galerkin method at particular points in the domain.

Finally, we shall define a method allowing us to calculate $\boldsymbol{\varphi}_h^n \in V_h$, an approximation to $\varphi_h(t_n)$ starting from $\boldsymbol{\varphi}_h^{n-1}$ (we limit ourselves to a two-level scheme). Then we can write

$$\boldsymbol{\varphi}_h^{n+1} = C_h(\Delta t)\boldsymbol{\varphi}_h^n + \Delta t\mathbf{f}_h^n, \quad \boldsymbol{\varphi}_h^0 = \boldsymbol{\varphi}_{0,h} \tag{32}$$

where we introduce the operator $C_h(\Delta t) \in \mathscr{L}(V_h)$ ($\mathscr{L}$ is the set of continuous linear mapping of V_h with values in V_h) and where $\mathbf{f}_h^n$ approximates $\mathbf{f}_h(t_n)$.

We shall always assume that the evolution problem (28) is well posed and there exists a projection R_h of E into V_h such that

$$\lim_{h\to 0} |R_h\boldsymbol{\varphi} - \boldsymbol{\varphi}|_E = 0 \quad \forall \boldsymbol{\varphi} \in E. \tag{33}$$

5.4. Convergence, consistency and stability

The first fundamental question is that of the convergence, when h and Δt tend to zero, of the sequence $\{\boldsymbol{\varphi}_h^n\}$, the solution (32), towards the function $\boldsymbol{\varphi}(t)$, the solution of (32). Let us restrict our consideration, for the moment, to the case where $\mathbf{f}(t) \equiv 0$.

Definition 1. The scheme defined by (32) will be called convergent if the condition

$$\boldsymbol{\varphi}_{0,h} \to \boldsymbol{\varphi}^0 \quad \text{as } h \to 0 \tag{34}$$

implies that

$$\boldsymbol{\varphi}_h^n \to \boldsymbol{\varphi}(t) \quad \text{as } \Delta t \to 0, \quad n \to \infty \quad \text{with } n\Delta t \to t \tag{35}$$

for all $t \in [0,t_0]$, $t_0 \in [0,t_f]$, where $\boldsymbol{\varphi}_h^n$ is defined by (32) and $\boldsymbol{\varphi}(t)$ is the solution of (28). All this holds for arbitrary $\boldsymbol{\varphi}^0$.

The study of the convergence of an approximation scheme involves two fundamental properties of the scheme, consistency and stability.

Definition 2. The scheme defined by (32) is called stable, if there exists a constant $K \geqslant 1$ independent of h and Δt such that

$$\|(C_h(\Delta t))^n R_h\|_{\mathscr{L}(E)} \leqslant K \quad \forall n, \Delta t \text{ satisfying } n\Delta t \leqslant t_0. \tag{36}$$

In Definitions 1 and 2 there occur two parameters h and Δt. It may be that the scheme is not stable (or convergent) unless Δt and h satisfy supplementary hypotheses of the type $\Delta t/h^{\alpha} \leqslant$ constant, $\alpha < 0$, in which case we call the scheme *conditionally stable*. If the scheme is stable for arbitrary h and Δt we say that it is *unconditionally stable*.

Definition 3. The scheme defined by (32) will be called consistent with Eq. (28) if there exists a subspace $Y \subset E$ dense in E, such that for every $\boldsymbol{\varphi}(t)$ which is a solution of (28) with $\boldsymbol{\varphi}^0 \subset Y$ (and $\mathbf{f} \equiv 0$) we have

$$\lim_{h\to 0, \Delta t \to 0} \left| \frac{C_h(\Delta t) R_h \boldsymbol{\varphi}(t) - \boldsymbol{\varphi}(t)}{\Delta t} - \mathscr{A}\boldsymbol{\varphi}(t) \right|_E = 0. \tag{37}$$

5.5. The Lax–Richtmayer equivalence theorem

We can now state the Lax–Richtmayer equivalence theorem (cf. [42,46,1,8]).

Theorem. *Suppose that the evolution problem* (28) *is well-posed for* $t \in [0, t_0]$ *and that it is approximated by the scheme* (32), *which we assume consistent. Then the scheme is convergent if and only if it is stable.*

The proof of the Lax–Richtmayer equivalence theorem for the case when the partial differential operator $\mathscr{A}$ in (28) is independent of $\boldsymbol{\varphi}$ can be found in [1].

Remark. *Let us consider the evolution problem* (28) *with*

$$\mathbf{f}(t, \boldsymbol{\varphi}) \neq 0 \tag{38}$$

and $\boldsymbol{\varphi}^0 = 0$, *and also the corresponding approximation* (32). *We have*

$$\boldsymbol{\varphi}_h^{n+1} = \Delta t \sum_{j=1}^{n} [C_h(\Delta t)]^{n-j} \mathbf{f}_h^j. \tag{39}$$

If $\mathscr{A}$ *is the infinitesimal generator of a semigroup* $\{\mathbb{F}(t)\}$ *we can write*

$$\boldsymbol{\varphi}(t) = \int_0^t \mathbb{F}(t-s)\mathbf{f}(s)\, \mathrm{d}s. \tag{40}$$

Under suitable hypotheses on the convergence of $\mathbf{f}_h^j$ to $\mathbf{f}(j\Delta t)$ we can show that expression (39) converges to (40) if the scheme is stable and consistent.

It is noteworthy that the spatial operator $\mathscr{A}$ defined by (12) has the same form as in thermo-elastodynamics while all dissipative effects generated by viscoplastic flow phenomena influence the process through the non-linear function $\mathbf{f}$. This fact has a very important result on the investigation of the application of the Lax–Richtmayer equivalence theorem to the evolution problem defined in Section 3.1. Based on the results obtained by Hughes at al. [11] and [12] for elastodynamics we can first prove that the evolution problem considered is well posed. Second, by investigation of the conditions for function $\mathbf{f}$ (cf. (17) and (18)) we can prove that expression (39) converges to (40) for our particular case when the function $\mathbf{f}$ has the form of Eq. (12). Indeed, assuming κ and Φ in the form (7) and (8) we can satisfy the conditions (17) and (18).

6. Numerical examples and results

In the numerical examples presented in this paper we study the behaviour of an axisymmetric specimen under dynamic tension. In general, we discuss two types of boundary conditions and applied loadings. Case A in Fig. 1 represents double-sided symmetrically applied velocities while case B reflects single-sided applied velocities with the fixed opposite edge. In the examples reported in the paper the velocities of displacements

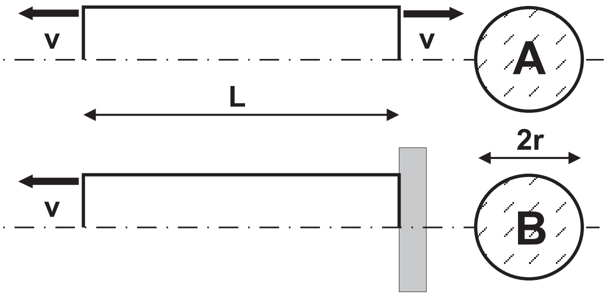

Fig. 1. Two types of specimen loadings: double-side, symmetric (A) and single-side, non-symmetric (B).

acting symmetrically on two opposite edges were changed from 0.5 to 20 m/s. The intensity of initial conditions obtains the final value after 0.01 s. For all the cases under consideration the process is finished when the elongation of the specimen is 2.5 mm. There was also activated the fracture criterion for material which was used in computations. We assumed that if the value of plastic equivalent strains (PEEQ) approached 100% the failure limit was reached. The specimen is of a length $L = 19.05$ mm and radius $r = 3.175$ mm. Only half of the specimen is presented in Fig. 1 and the arrows with indicated velocities v symbolically describe the equal displacements of all the points at the edges. In the computations the data were accepted as follows: Young modulus $E = 200.000$ MPa, Poisson ratio $\nu = 0.3$, yield limit $\sigma_p = 1634$ MPa for initial temperature which changes non-linearly (softens) down to 1006 MPa for the rise of temperature up to 610°C, mass density $\rho = 7850$ kg/m^3 and the relaxation time of mechanical perturbances which changed from $T_m = 0.025$ s for initial temperature 20°C to 0.01 s for elevated temperature up to 80°C. The problem was treated as an adiabatic case with specific heat 460 J/kg K and heat fraction 0.9.

6.1. Symmetric loading – case A

First, let us take some computational experiments for symmetrically applied loadings at both ends. In the following figures, Figs. 2–6, the changes of plastic equivalent strains, their development as well as the changes of reactions and temperatures are reported. In Fig. 2 we present several stages of growth of PEEQ

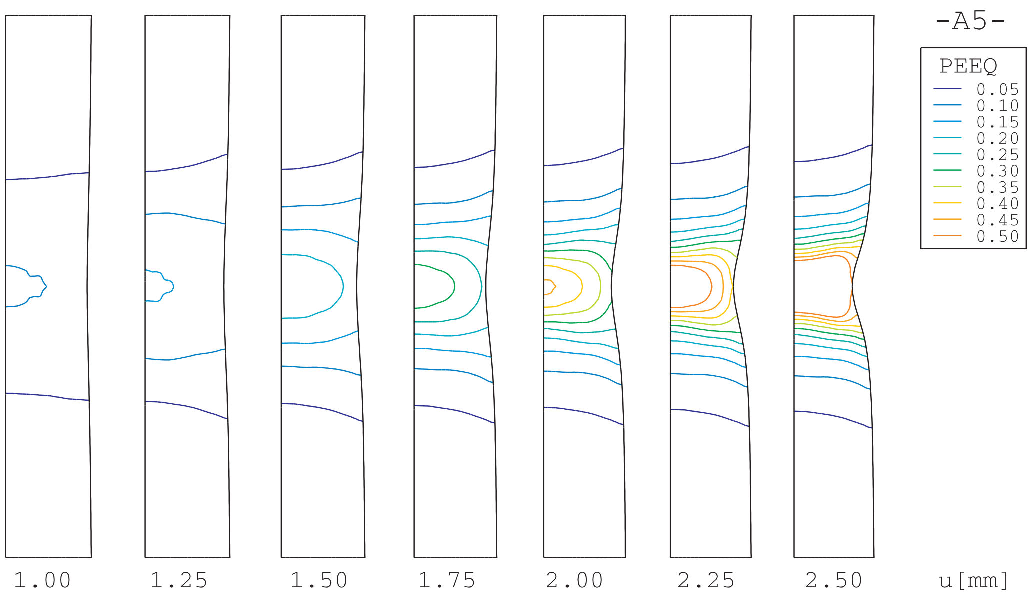

Fig. 2. The development of plastic equivalent strains under double-side velocity 5 m/s (A5) for different total elongation u of the specimen.

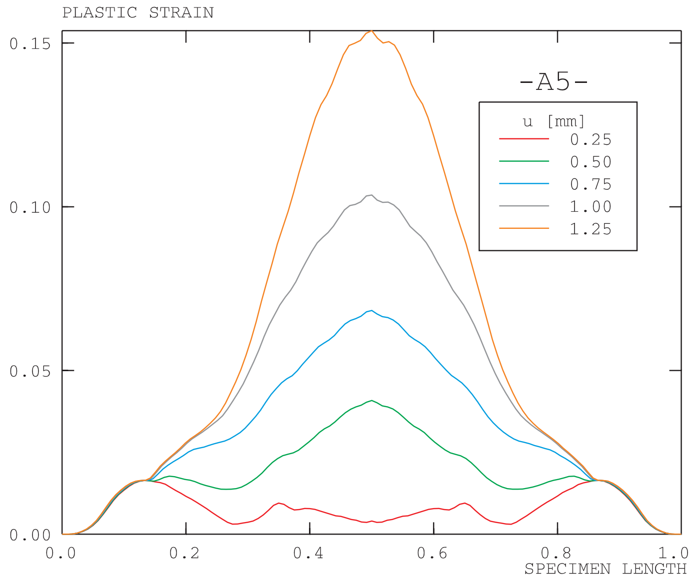

Fig. 3. Plastic equivalent strain along the specimen axis for different total elongation.

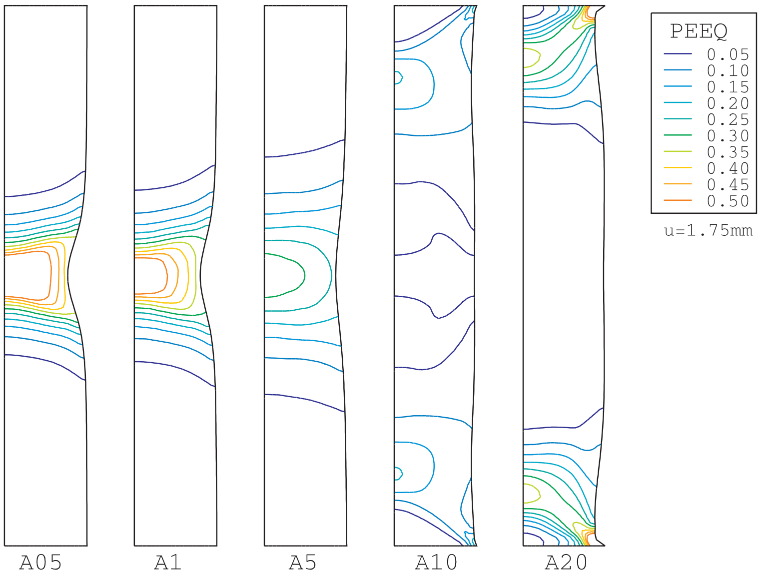

Fig. 4. The contours of plastic equivalent strain for the total elongation of the specimen $u = 1.75$ mm for different double-side velocities (A).

for different total elongations. The reached values of PEEQ locally approximate 50% for total elongations of order 10–12%. Fig. 3 presents the changes of PEEQ along the axis of symmetry of the specimen for different elongations. The level of diffusion of the zone of localization significantly depends on the constitutive parameter, namely the relaxation time T_m. For shorter T_m the width of the localized zone is smaller. This kind of study was presented by [7,34].

The contour plots of PEEQs obtained for different velocities of loading (0.5, 1.0, 5.0, 10.0 and 20.0 m/s) are visualized in Fig. 4 for the same total elongation $u = 1.75$ mm. It is clearly visible that for different velocities the places of strain localization appear always symmetrically but with different intensity and in

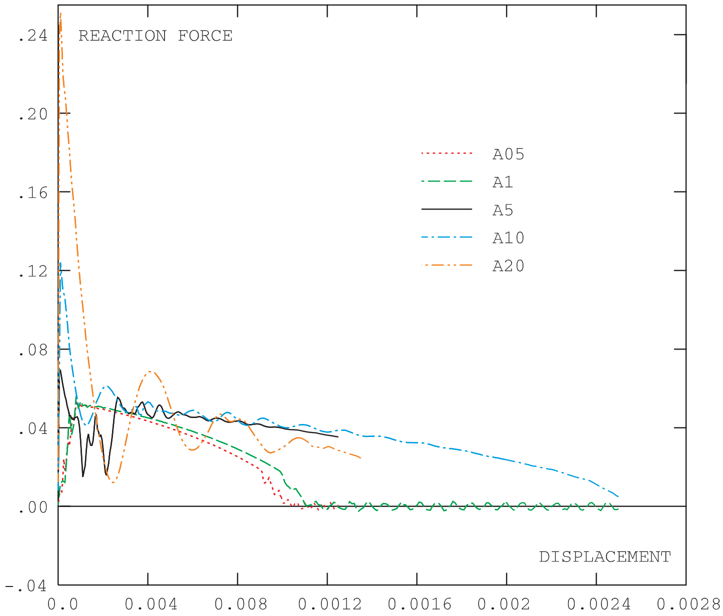

Fig. 5. Reaction force versus displacement for different double-side velocieties.

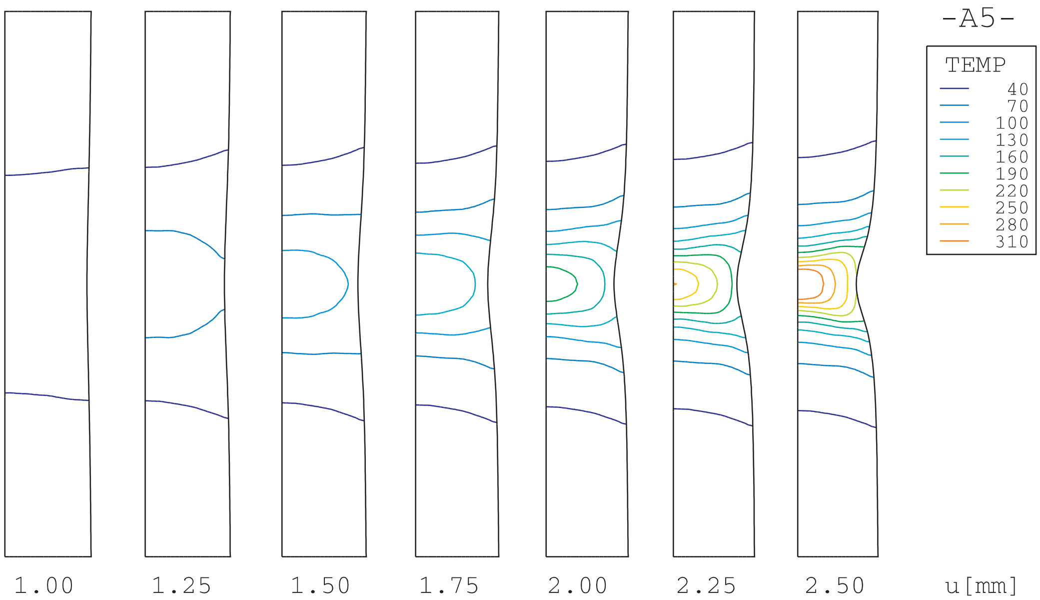

Fig. 6. The development of temperature under double-side velocity 5 m/s (A5) for different total elongation u of the specimen.

different places (in the middle or for higher loading velocities close to the loaded edges). In Fig. 5 there are the plots of reactions which act at the loaded sides as a function of displacements. The wave character of this reaction is evident. Finally, in Fig. 6 one can observe the changes of temperature that take place during the adiabatic process of deformations with the velocity loading $v = 5.0$ m/s for different total elongation of the specimen.

This important observation confirms that the place of localization is chosen only as an effect of waves interaction and significantly depends on the initial conditions.

6.2. Unsymmetric loading – case B

Two choice of places of plastic strain localization for single-sided loading with the opposite side fixed are even more sensitive to the initial conditions than in previous symmetric cases. In Fig. 7 we present the development of PEEQ in the specimen under the velocity $v = 5.0$ m/s. The process is controlled by the velocity that acts at the top edge of the axisymmetrical specimen. Fig. 8 shows the changes of PEEQ for the same velocity and different elongations along the symmetry axis. One can observe that at the very beginning of deformations for quite small elongations (of order 1%), there are two possible places where the deformations could localize. However, later only one cross section, closer to the fixed edge becomes the localization zone while the other place of intense straining unloads.

In Fig. 9 we show the places of localization for different velocities between $v = 0.5$ and $v = 20.0$ m/s. It is easy to expect that for quasistatic cases (very slow processes) the localized zone would appear in the middle of the specimen. For higher velocities (between 5.0 and 10.0 m/s) the localization appears in different places depending on the interaction of waves. For the loading velocities higher than a critical value the localization appears close to the loaded edge. The same phenomena are also recognized in experiments.

Fig. 10 presents the wave character of showing the reaction as a function of elongations (here directly displacements). The changes of the temperature field in adiabatic process under the velocity loading with the intensity of $v = 5.0$ m/s are presented in Fig. 11 as a function of total displacements. The temperature rise is close to that which is observed in laboratory experiments.

At the end of Fig. 12 there are the vector plots of velocities of particles in the specimen for different stages of the process. The longitudinal waves propagate with the elastic speed. In Fig. 12 the crucial role of reflection of waves and its interaction is visible. In the vicinity of the place of localization the speed of waves is almost equal to zero. The vector plot (arrows) shows the directions of the particle movements and the length of arrows reflects their values. In the areas where the localization appears the velocities and also the accelerations are close to zero.

It has been observed (cf. Figs. 4 and 9 for initial velocities 10 and 20 m/s) that for the strain rate in the range of $10^3 - -10^4$ s^{-1} inertial effects are important because of the propagation of dispersive waves that cause heterogeneity in the distribution of stress and deformation at the initial stages of the test. This phenomenon has also been noticed by Nemes and Eftis [23] and it is in agreement with experimental observations performed by Regazzoni and Montheillet, and Rajendran and Bless [39,38].

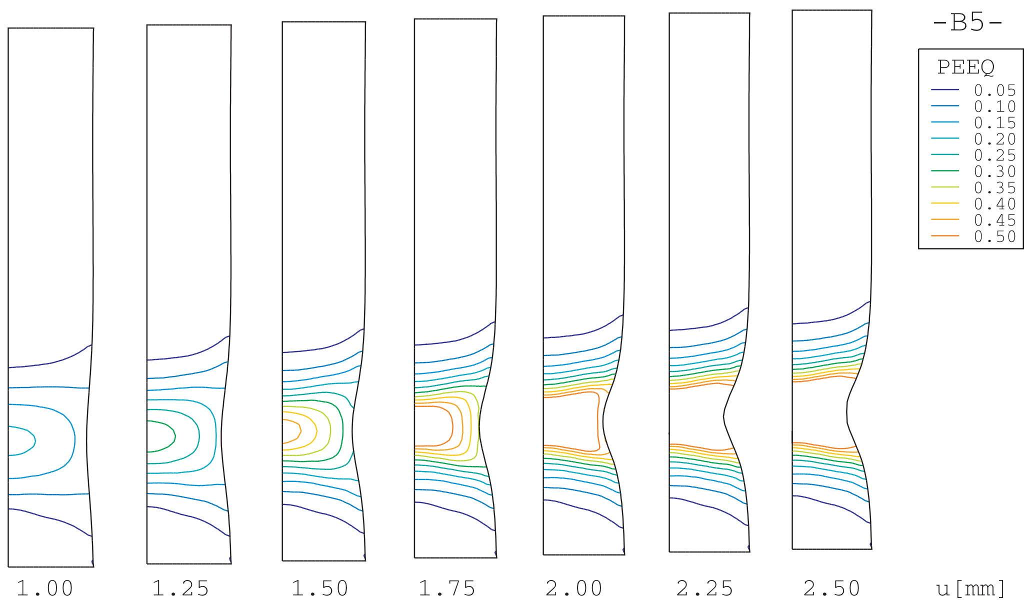

Fig. 7. The development of plastic equivalent strains under single-side velocity 5 m/s (B5) for different total elongation u of the specimen.

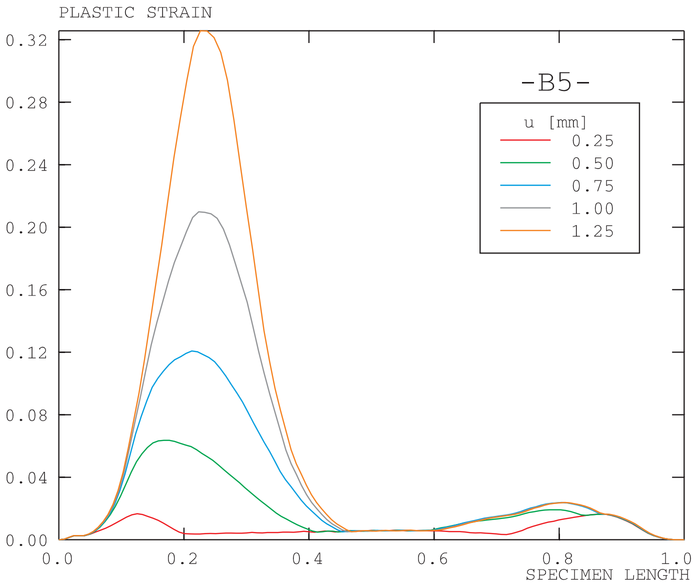

Fig. 8. Plastic equivalent strain along the specimen axis for different total elongation.

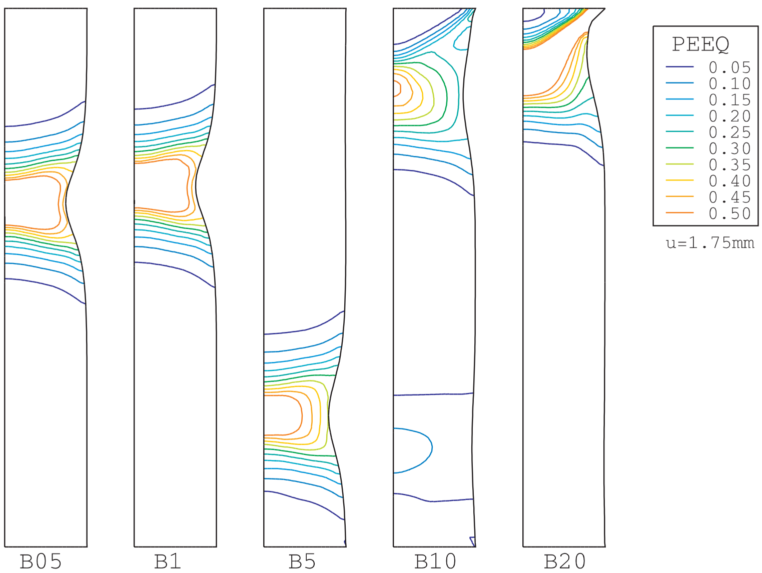

Fig. 9. The contours of plastic equivalent strain for the total elongation of the specimen $u = 1.75$ mm for different single-side velocities (B).

7. Final comments

The main important physical aspects of an elastic–viscoplastic medium proposed are as follows: (i) the adiabatic thermal softening associated with high strain rate inelastic deformations; (ii) strain hardening–softening effect; (iii) dispersive and dissipative wave motion; (iv) a length-scale parameter is implicitly introduced into the dynamical initial-boundary value problem; (v) strain-rate sensitivity.

The numerical simulations of the evolution problems have shown that for dynamically imposed loading the inhomogeneous fields of stress and deformation are caused by the propagation of waves and the

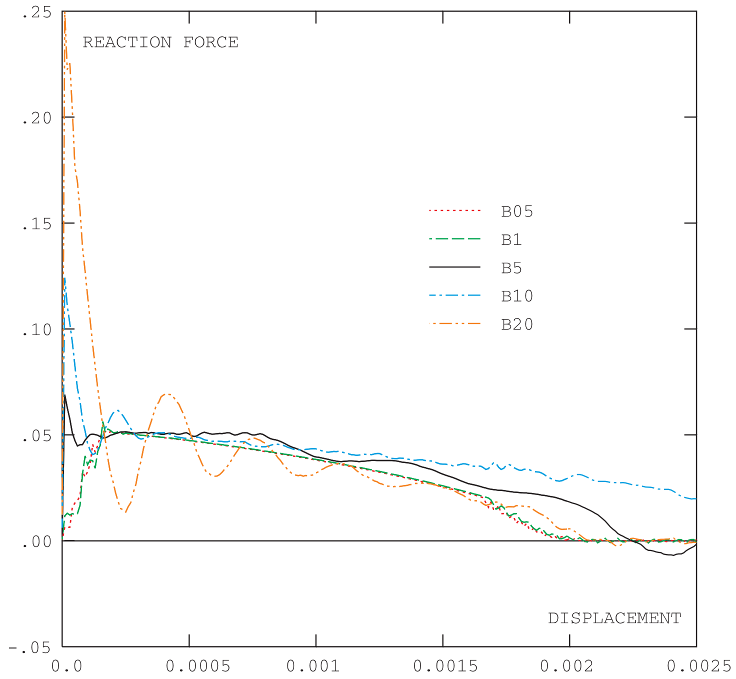

Fig. 10. Reaction force versus displacement for different single-side velocieties.

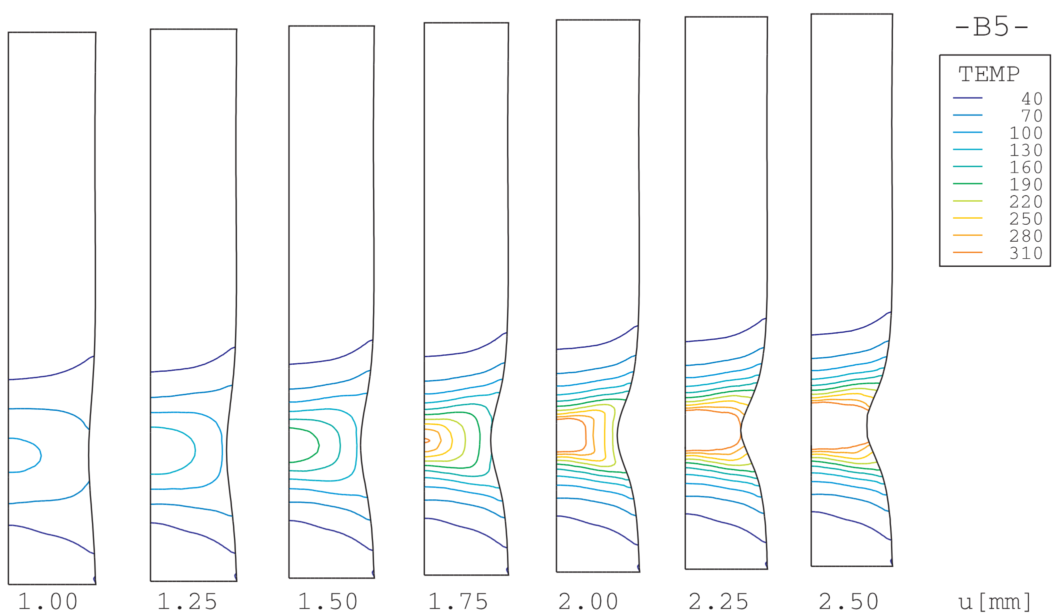

Fig. 11. The development of temperature under single-side velocity 5 m/s (B5) for different total elongation u of the specimen.

reflection of waves. This interaction of waves induced necking at different locations along the specimen depending upon the strain rate imposed. The phenomenon of localization of plastic deformation occurs without imposition of any geometrical, thermal or material imperfections. In each of the numerical examples considered due to different boundary conditions the evolution of the necking looks different. Propagative waves have dispersive and dissipative nature and this fact has fundamental influence on the development of localization of plastic deformation in a mode of necking.

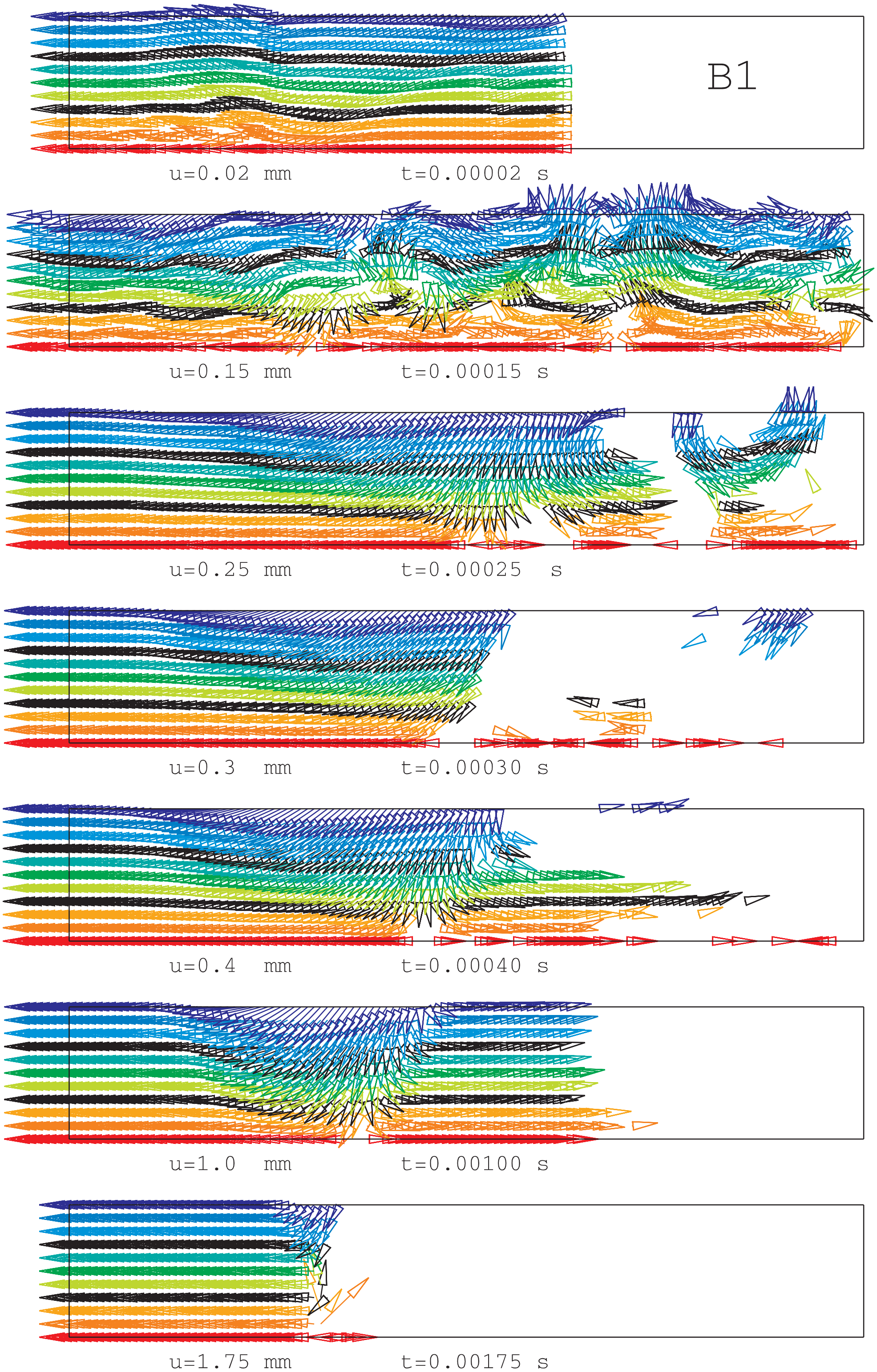

Fig. 12. The development of velocity vector under single-side velocity 1 m/s (B1) for different total elongation u.

The numerical simulations are able to provide graphic illustrations (cf. Figs. 2–12) which proved that the interactions and reflections of dispersive, dissipative waves generate the time evolution of the spatial localization and the intensification of stress and equivalent plastic deformation in the developing neck.

The temperature rise computed in the diffused neck confirmed the assumption that the evolution process has to be treated as adiabatic.

Acknowledgements

The paper has been partly prepared within the research programme sponsored by the Committee of Scientific Research under Grant 3 P 404 031 07.

References

[1] R. Dautray, J.L. Lions, Mathematical Analysis and Numerical Methods for Science and Technology, vol. 6, Evolution Problems II, Springer, Berlin, 1993.
[2] M.A. Dowaikh, R.W. Ogden, Interfacial waves and deformations in pre-stressed elastic media, Proc. Roy. Soc. London A 433 (1991) 313–328.
[3] M.K. Duszek, P. Perzyna, The localization of plastic deformation in thermoplastic solids, Internat. J. Solids Struc. 27 (1991) 1419–1443.
[4] M.K. Duszek-Perzyna, P. Perzyna, Analysis of the influence of different effects on criteria for adiabatic shear band localization in inelastic solids, Material Instabilities: Theory and Applications AMD, vol. 183/MD–vol. 50, 1994, ASME, pp. 59–85.
[5] M.K. Duszek-Perzyna, P. Perzyna, Acceleration waves in analysis of adiabatic shear band localization, in: J.L. Wegner, F.R. Norwood (Eds.), Non-linear Waves in Solids, Proceedings of the IUTAM Symposium, August 15–20, 1993, Victoria, Canada, ASME 1995, pp. 128–135.
[6] A. Glema, W. Kakol, T. Łodygowski, Numerical modelling of adiabatic shear band formation in a twisting test, Eng. Trans. 45 (3–4) (1997) 419–431.
[7] A. Glema, R. Łodygowski, P. Perzyna, Localization of plastic deformations as a result of wave interaction, Euromech Colloquium 385 on Inelastic Analysis of Structures under Variable Loads: Theory and Engineering Applications, Aachen, Germany, 8–11 September 1998 (in print in proceedings).
[8] B. Gustafsson, H.O. Kreiss, J. Oliger, Time-Dependent Problems and Difference Methods, Wiley, New York, 1995.
[9] J. Hadamard, Lecons sur la propagation des ondes et les equations de l'hydrodynamique, Chap. 6, Paris, 1903.
[10] R. Hill, Acceleration wave in solids, J. Mech. Phys. Solids 10 (1962) 1–16.
[11] T.J.R. Hughes, T. Kato, J.E. Marsden, Well-posed quasilinear second-order hyperbolic systems with applications to non-linear elastodynamics and general relativity, Arch. Rat. Mech. Anal. 63 (1977) 273–294.
[12] T.J.R. Hughes, J.E. Marsden, Classical elastodynamics as a linear symmetric hyperbolic systems, J. Elasticity 8 (1978) 97–110.
[13] I.R. Ionescu, M. Sofonea, Functional and Numerical Methods in Viscoplasticity, Oxford, 1993.
[14] T. Łodygowski, On avoiding of spurious mesh sensitivity in numerical analysis of plastic strain localization, Comput. Assisted Mech. Eng. Sci. 2 (1995) 231–248.
[15] T. Łodygowski, M. Lengnick, P. Perzyna, E. Stein, Viscoplastic numerical analysis of dynamic plastic strain localization for a ductile material, Archives Mech. 46 (1994) 1–25.
[16] T. Łodygowski, P. Perzyna, Numerical modelling of localized fracture of inelastic solids in dynamic loading processes, Internat. J. Num. Meth. Eng. 40 (1997a) 4137–4158.
[17] T. Łodygowski, P. Perzyna, Localized fracture in inelastic polycrystalline solids under dynamic loading processes, Internat. J. Damage Mech. 6 (1997b) 364–407.
[18] J. Mandel, Conditions de stabilité et postulat de Drucker, in: J. Kravchenko, P.M. Sirieys (Eds.), Rheology and Soil Mechanics, Springer, New York, 1966, pp. 58–68.
[19] J.E. Marsden, T.J.R. Hughes, Mathematical Foundations of Elasticity, Prentice-Hall, Englewood Cliffs, NJ, 1983.
[20] A. Needleman, Material rate dependence and mesh sensitivity in localization problems, Comput. Meth. Appl. Mechs. Eng. 67 (1988) 69–85.
[21] A. Needleman, Dynamic shear band development in plane strain, J. Appl. Mech. 56 (1989) 1–9.
[22] A. Needleman, M. Ortiz, Effects of boundaries and interfaces on shear-band localization, Internat. J. Solids Struc. 28 (1991) 859–877.
[23] J.A. Nemes, J. Eftis, Constitutive modelling on the dynamic fracture of smooth tensile bars, Internat. J. Plasticity 9 (1993) 243–270.
[24] J.A. Nemes, J. Eftis, P.W. Randles, Viscoplastic constitutive modelling of high strain-rate deformation, material damage and spall fracture, J. Appl. Mech. 57 (1990) 282–291.
[25] R.W. Ogden, Non-linear effects associated with waves in pre-stressed elastic solids near bifurcation points, in: J.L. Wegner, F.R. Norwood (Eds.), Non-linear Waves in Solids, Proceedings of the IUTAM Symposium, August 15–20, 1993, Victoria, Canada, ASME 1995, pp. 109–113.

[26] N.S. Ottosen, K. Runesson, Acceleration waves in elasto-plasticity, Internat. J. Solids Struc. 28 (1991) 135–159.
[27] P. Perzyna, The constitutive equations for rate sensitive plastic materials, Quart. Appl. Math. 20 (1963) 321–332.
[28] P. Perzyna, Thermodynamic theory of viscoplasticity, Advances Appl. Mech. 11 (1971) 313–354.
[29] P. Perzyna, Constitutive modelling of dissipative solids for postcritical behaviour and fracture, ASME J. Eng. Mater. Technol. 106 (1984) 410–419.
[30] P. Perzyna, Internal state variable description of dynamic fracture of ductile solids, Internat. J. Solids Struc. 22 (1986) 797–818.
[31] P. Perzyna, Adiabatic shear band localization fracture of solids in dynamic loading processes, in: J. Harding (Ed.), Proceedings of the International Conference on Mechanical and Physical Behaviour of Materials under Dynamic Loading, Oxford, September 26–30, 1994, Les Editions de Physique Le Ulis 1994, pp. 441–446.
[32] P. Perzyna, Instability phenomena and adiabatic shear band localization in thermoplastic flow processes, Acta Mechanica 106 (1994) 173–205.
[33] P. Perzyna, Interactions of elastic–viscoplastic waves and localization phenomena in solids, in: J.L. Wegner, F.R. Norwood (Eds.), IUTAM Symposium on Non-linear Waves in Solids, August 15–20, 1993, Victoria, Canada, ASME 1995, pp. 114–121.
[34] P. Perzyna, Dynamic localized fracture in inelastic solids, in: Damage Mechanics in Engineering Materials, G.Z. Voyadjis (Ed.), Elsevier, Amsterdam, 1998, pp. 183–202.
[35] P. Perzyna, M.K. Duszek-Perzyna, Phenomenological modelling of adiabatic shear band localization fracture of solids in dynamic loading processes, in: M.H. Aliabadi, A. Carpinteri, S. Kalisky, D.J. Cartwright (Eds.), Localized Damage III; Computer-Aided Assessment and Control, Computational Mechanics Publications, Southampton, 1994, pp. 579–588.
[36] P. Perzyna, W. Wojno, Interaction of dispersive waves and localization phenomena in damaged solids, Arch. Mechanics 50, (submitted for publication).
[37] J.H. Prevost, B. Loret, Dynamic strain localization in elasto- (visco-plastic) solids, II. Plane strain examples, Comput. Meth. Appl. Mech. Eng. 83 (1990) 247–294.
[38] A.M. Rajendren, S.J. Bless, High strain rate material behaviour, in: AFWAL–TR-85-4009, Materials Laboratory, Air Force Wright Aeronautical Laboratories, Wright–Patterson Air Force Base, Ohio, 1985.
[39] G. Regazzoni, F. Montheillet, Influence of strain rate on the flow stress and ductility of copper and tantalum at room temperature, in: J. Harding (Ed.), Proceedings of the Third International Conference on the Mechanical Properties of Materials at High Rates, vol. 70, The Institute of Physics, 1984, pp. 63–70.
[40] J.R. Rice, The localization of plastic deformation, in: W.T. Koiter (Ed.), Theoretical and Applied Mechanics, North-Holland, Amsterdam, 1976, pp. 207–220.
[41] R.D. Richtmyer, Principles of Advance Mathematical Physics, Springer, New York, 1978.
[42] R.D. Richtmyer, K.W. Morton, Difference Methods for Initial-value Problems, Wiley, New York, 1967.
[43] H.C. Simpson, S.J. Spector, On the positivity and the second variation in finite elasticity, Arch. Rat. Mech. Anal. 32 (1989) 369–399.
[44] L.J. Sluys, Wave Propagation, Localization and Dispersion in Softening Solids, Doctoral Thesis, Delft University Press, Delft, 1992.
[45] L.J. Sluys, J. Bolck, R. de Borst, Wave propagation and localization in viscoplastic media, in: D.R.J. Owen, E. Onate, E. Hinton (Eds.), Proceedings of the Third International Conference on Computational Plasticity, Fundamentals and Applications, Barcelona, April 6–10, 1992, Pineridge Press, Swansea, 1992, pp. 539–550.
[46] G. Strang, G.J. Fix, An Analysis of the Finite Element Method, Prentice-Hall, Englewood Cliffs, NJ, 1973.
[47] Z. Suo, M. Ortiz, A. Needleman, Stability of solids with interfaces, J. Mech. Phys. Solids 40 (1992) 613–640.
[48] S.A. Thau, Linear dispersive waves, in: S. Leibovich, A.R. Seebass, (Eds.), Non-linear Waves, Cornell University Press, Ithaca, 1974, pp. 44–81.
[49] T.Y. Thomas, Plastic Flow and Fracture of Solids, Academic Press, New York, 1961.
[50] C. Truesdell, General and exact theory of waves in finite elastic strain, Arch. Rat. Mech. Anal. 19 (1965) 263–296.
[51] C. Truesdell, W. Noll, The non-linear field theories, in: Handbuch der Physik, Band III/3, Springer, Berlin, 1965, pp. 1–579.
[52] W.M. Wang, Stationary and Propagative Instabilities in Metals – A Computational Point of View, Doctoral Thesis, Delft University Press, Delft, 1997.
[53] W.M. Wang, L.J. Sluys, R. deBorst, Interaction between material length scale and imperfection size for localization phenomena in viscoplastic media, European J. Mech. 15 (1996) 447–464.
[54] G.B. Whitham, Linear and Non-linear Waves, Wiley, New York, 1974.
[55] G.B. Whitham, Dispersive waves and variational principles, in: S. Leibovich, A.R. Seebass (Eds.), Non-linear Waves, Cornell University Press, Ithaca, 1974, pp. 139–169.